Experimental demonstration of multigranularity switching between optical DFT-spread-OFDM and Nyquist superchannel

Rui Ding (丁瑞)*, Tingting Zhang (张婷婷), and Fan Zhang (张帆)**

State Key Laboratory of Advanced Optical Communication Systems & Networks, Peking University, Beijing 100871, China

**Corresponding author: onlydingrui@163.com; **corresponding author: fzhang@pku.edu.cn*

Received May 13, 2014; accepted July 25, 2014; posted online October 28, 2014

We experimentally investigate multigranularity optical subband switching functionality between two superchannels with slight error vector magnitude penalty. One is 4×39 Gb/s polarization-division-multiplexed (PDM) quadrature phase shift keying discrete Fourier transform spread orthogonal frequency division multiplexing (DFT-spread-OFDM) superchannel with 12.5 GHz band spacing. The other is 8×29 Gb/s PDM-16-quadrature amplitude modulation Nyquist pulse shaping superchannel with 6.25 GHz band spacing. To the best of our knowledge, this is the first time that optical switching functionality for individual band between different superchannels with multigranularity is realized.

OCIS codes: 060.0060, 060.1660, 060.2360.

DOI: 10.3788/COL201412.110604.

Spectrally efficient transmission technologies are required for the future optical network. So far, two strategies are introduced to achieve high spectral efficiency (SE) with reasonable signal processing complexity. The first scheme is coherent optical orthogonal frequency-division multiplexing (CO-OFDM). The second one is based on Nyquist wavelength-division multiplexing (WDM).

CO single-carrier frequency-division multiplexing (SCFDM) has been proposed in CO systems[1], which is a modified form of OFDM and has been used in uplink single-carrier frequency-division-multiple-access (SC-FDMA) scheme for the Long Term Evolution of cellular systems by the Third Generation Partnership Project (3GPP)[2]. Comparing with OFDM, the SCFDM has similar tolerances to linear dispersion impairments, but achieves better tolerances to nonlinear impairments[1,3,4]. Zhao *et al.*[5] showed that 1.08 Tb/s polarization-division-multiplexed (PDM) CO-SCFDM signals transmit over 3170 km standard single-mode fiber (SSMF). If generated in frequency domain, SCFDM is also called discrete Fourier transform spread (DFT-S)-OFDM[6].

With similar rectangle-like spectrum, Nyquist pulse shaping signals have comparable SE to OFDM under the same modulation format. Zheng *et al.*[7] showed 1.76 Tb/s Nyquist PDM-16-quadrature amplitude modulation (QAM) signal to transmit over 714 km SSMF with a SE of 7.06 b/s/Hz. Zhou *et al.*[8] showed successful transmission of 5×450 Gb/s Nyquist PDM 32QAM WDM signal on the 50 GHz ITU-T Grid with a SE of 8.4 b/s/Hz.

The significant change in transmission technique has much influence on future optical network. Reconfigurable optical add/drop multiplexer (ROADM) functionality has been shown on OFDM or SCFDM superchannel[9,10]. In previous work[11], we have shown that Nyquist superchannel is also a good candidate for ROADM functionality in dynamic optical networks. In future optical network with mixed optical signal, it is inevitable to switch between different superchannel systems.

Ding *et al.*[12] conducted preliminary investigation on multigranularity optical subband switching function performed between Nyquist and DFT-S-OFDM superchannel systems, but with large performance penalty. In this letter, we optimize the guard-band for both superchannel systems. Adopting steeper optical filter, we show multigranularity optical subband switching functionality on a 12.5 GHz frequency grid with only a slight error vector magnitude (EVM) penalty. The 12.5 GHz grid covers one subband in DFT-S-OFDM superchannel and two subbands in Nyquist superchannel.

The DFT-S-OFDM superchannel, we considered in this experiment, comprises four subbands with 12.5 GHz band spacing. The total baud rate of each subband is 12 Gbaud. The fast Fourier transform length is 128. Figure 1 shows the back-to-back performance of 2nd DFT-S-OFDM band with different guard subcarriers. In error-free systems, performance can be measured with the EVM value[13]. In this letter, we transform the linear EVM to dB domain by operator $-10\times\log10$.

We can see that larger guard band guarantees better performance at the cost of lower SE. 22 guard subcarriers is a trade-off between the performance and SE. Thus, the net baud rate for each DFT-S-OFDM subband is 9.9375 Gbaud.

At the transmitter, the mapped quadrature phase shift keying (QPSK) signals are grouped into blocks with 102 symbols each, and 4 pilots are time-domain multiplexed into the block. The signal is then transformed into frequency domain by 106-point DFT and 11 image subcarriers are added at both sides. After subcarrier mapping, a 128-point inverse DFT transforms the signal to time domain. Both cyclic prefix (CP) and cyclic suffix (CS) with a length of five symbols are inserted in each data block before transmission.

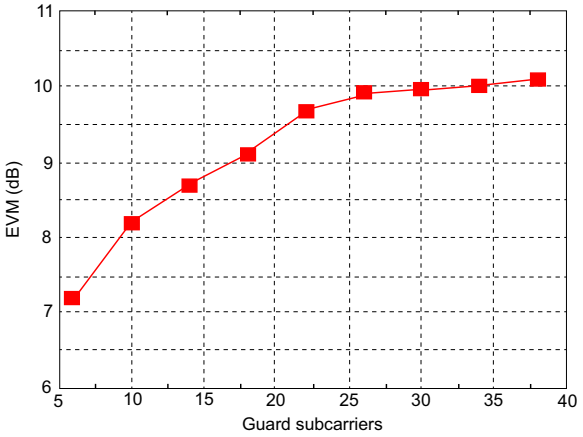

Fig. 1. Optimization of the guard band for DFT-S-OFDM superchannel.

At the receiver, firstly, CP and CS are removed, and then the 128-point DFT transforms the signals into frequency domain to remove guard subcarrier, and channel equalization is jointly performed for both polarizations.

The Nyquist superchannel comprises eight subbands with 6.25 GHz band spacing. To satisfy the guard band requirement of DFT-S-OFDM superchannel, which is shown in Fig. 2, we set the baud rate as 3.6875 Gbaud/s.

At the transmitter, the information data would be firstly mapped into 16-QAM format and then packed into blocks with 126 symbols each. After inserting two pilots in the data, the preamble including training sequences of four 127-bit M-sequences are added to the front of each frame.

At the receiver, training sequences are picked up for channel estimation in frequency domain, and the finite impulse response filter-based channel equalization is performed in time domain[7]. Table 1 shows the detailed parameters of Nyquist and DFT-S-OFDM superchannel.

Figure 3 shows the experimental setups demonstrating the multigranularity optical subband switching functionality.

In previous work[12], Finisar Waveshaper 4000s is used to perform subband selective switch functionality. The waveshaper has the ability to divide optical spectrum into arbitrary spectral slices and provide good control of filter amplitude. Another tunable optical filter with adjustable bandwidth called Yenista XTM-50 is also available. In the experiment, the waveshaper can perform as a band-pass or band-stop filter with a 10 GHz minimum bandwidth. XTM-50 can only be used as a band-pass filter, but with a 6.25 GHz minimum bandwidth.

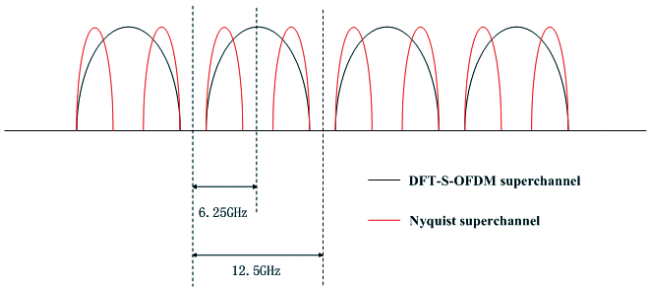

Fig. 2. Schematic diagram of spectrum for two superchannel systems.

Table 1. Details of Nyquist /DFT-S-OFDM Superchannel

Parameter	DFT-S-OFDM	Nyquist
Number of Subbands	4	8
Modulation Format	PDM-QPSK	PDM-16-QAM
Baud Rate (Gbaud)	9.9375	3.6875
Subband Spacing (GHz)	12.5	6.25
SE (b/s/Hz)	3.18	4.64
Total Capacity (Gb/s)	156	232

In the express path, which is shown in Figs. 3(a) and (b), the waveshaper is configured as an all-pass filter. The EVM value of every subband in the express path is calculated as a reference for comparison with switching path. In Fig. 3(c), Nyquist superchannel is divided into two groups by Waveshaper1 and XTM-50. One group comprises subbands 1, 2, 5, 6, 7, and 8, the other contains subbands 3 and 4. The Waveshaper2, with the help of XTM-50, divides the DFT-S-OFDM superchannel into two groups, which are one with band 2 and the other with bands 1, 3, 4. Then

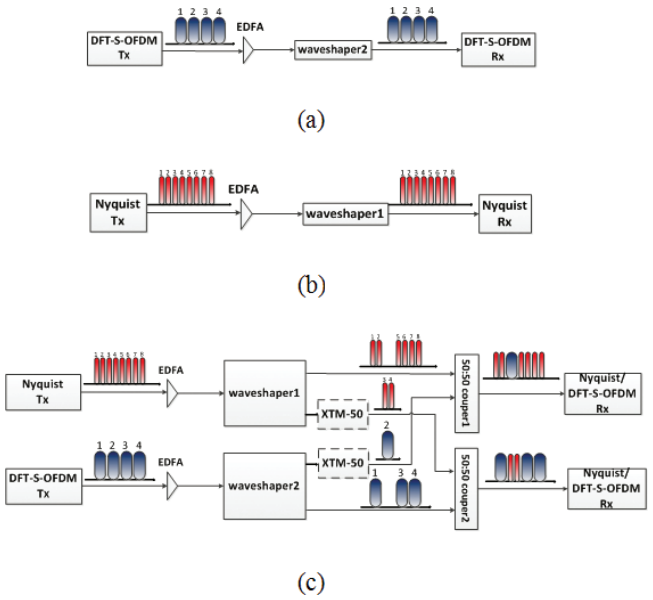

Fig. 3. Experiment setup of optical switching: (a) Express path for DFT-S-OFDM superchannel, (b) express path for Nyquist superchannel, and (c) subbands switching path.

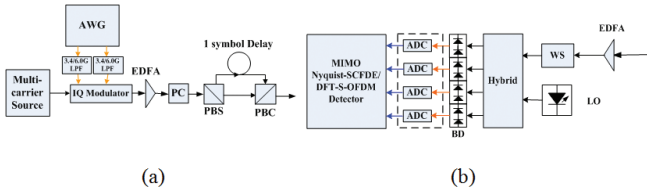

Fig. 4. Experiment setup of two superchannels: (a) transmitter and (b) receiver.

the four subband signals are interchanged with two 3dB couplers, respectively. The EVM value of each subband of two superchannels after switching is calculated.

The detailed setup of transmitter for both superchannels is shown in Fig. 4(a). For the Nyquist superchannel, the multicarrier source comprises eight lasers with 6.25 GHz band spacing. For the DFT-S-OFDM superchannel, the multicarrier source comprises four lasers with 12.5 GHz band spacing. The lasers we used are EXFO IQS-636 with ~100 kHz linewidth and ±2.5 GHz frequency accuracy. To ensure the match of laser frequency and center frequency of optical filter, an OSA with 0.01-nm resolution is used to monitor output signal of the optical filters all the time. A Tektronix arbitrary waveform generator (AWG7122B) operating at 7.375 GS/s (with 2-point DAC upsampling) and 12 GS/s (with 1-point DAC sampling) is used to generate baseband electrical Nyquist signals of 3.6875 Gbaud and DFT-S-OFDM signals of 12 Gbaud, respectively. Root-raised-cosine filters with a roll-off factor of 0.07 are chosen for Nyquist pulse shaping in this experiment. Two analog electric low-pass filters (ELPFs) with 3 dB bandwidth of 3.4 or 6 GHz are chosen for anti-aliasing filtering on Nyquist and DFT-S-OFDM signals. The PDM emulator consists of a polarization controller (PC), a polarization beam splitter/combiner (PBS/PBC), and a tunable optical delay line. The delay of the optical delay line is exactly one Nyquist or DFT-S-OFDM block. Therefore at the output of the transmitter, we can obtain an optical Nyquist PDM-16-QAM superchannel including eight subbands, each carrying a gross capacity of 29 Gb/s. The DFT-S-OFDM PDM-QPSK superchannel includes four subbands, each carrying 39.75 Gb/s.

At the receiver, as shown in Fig. 4(b), the received signal was firstly filtered by a waveshaper as a band-pass

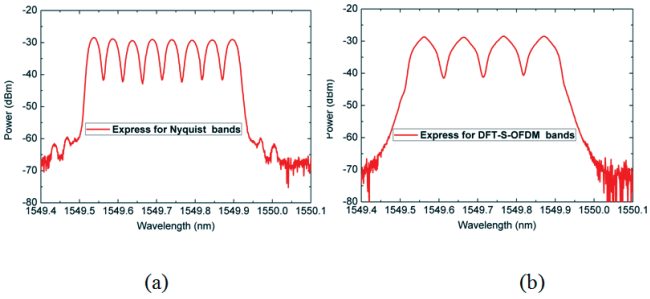

Fig. 5. Optical spectra in express path: (a) Nyquist superchannel and (b) DFT-S-OFDM superchannel.

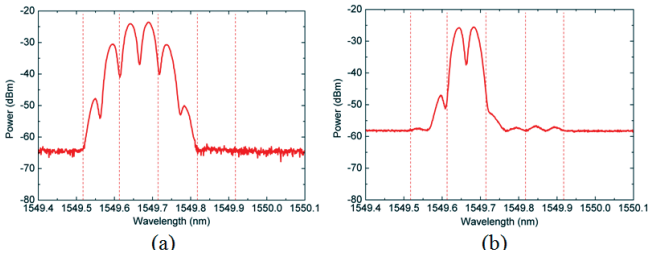

Fig. 6. Spectra of Nyquist superchannel filtered by different optical filters: (a) Waveshaper and (b) XTM-50.

filter. Then the signal is sent into an optical hybrid to interface with a local oscillator (LO) before detected by four balanced detectors (BDs). The signals are sampled by a real-time digital storage oscilloscope (Tektronix DPO72004B) at 50 GS/s for off-line processing.

The optical spectra of signals in the express path are shown in Figs. 5(a) and (b). Nyquist superchannel occupies 0.4 nm bandwidth with two subbands in each 12.5 GHz grid, While the DFT-S-OFDM superchannel occupies the same bandwidth with only one subband in each 12.5 GHz grid. The resolution is set as 0.01-nm for all the optical spectra in the experiment.

The switching functionality will induce a penalty for the subbands due to the imperfect filtering characteristics of optical filter. Figure 6 shows the spectra of bands 3 and 4 divided by Waveshaper 4000s on a minimum bandwidth 10 GHz and XTM-50 on a less than 10 GHz bandwidth, respectively. The residual signals of adjacent bands beside Nyquist bands 3 and 4 will induce same frequency interference on DFT-S-OFDM bands 1 and 3. We can see that the extinction ratio of the adjacent band is less than 10 dB for Waveshaper 4000s and larger than 20 dB for XTM-50. The constellation diagram for DFT-S-OFDM band 3 after switching is shown in Fig. 7. We use XTM-50 to replace Waveshaper 4000s as the band-pass filter in the experiment. But we still use Waveshaper 4000s as the band-stop filters.

Figures 8 and 9 show the signal spectrum before and after coupler 1 or coupler 2, respectively. Figures 8(b) and 9(a) show the output of band-pass filter realized by XTM-50. It can be observed that the residual signals

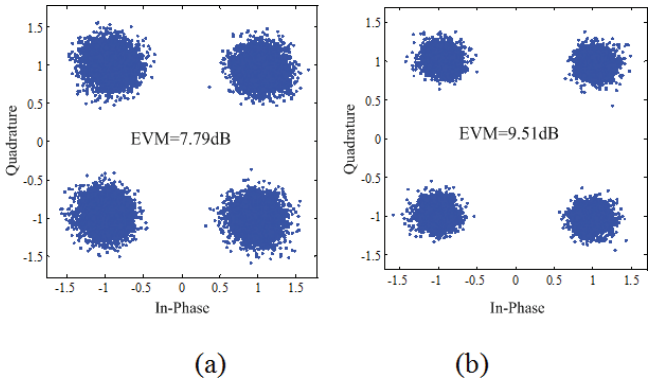

Fig. 7. Constellation diagram for DFT-S-OFDM band 3 adopting different band-pass optical filters: (a) Waveshaper 4000s and (b) XTM-50.

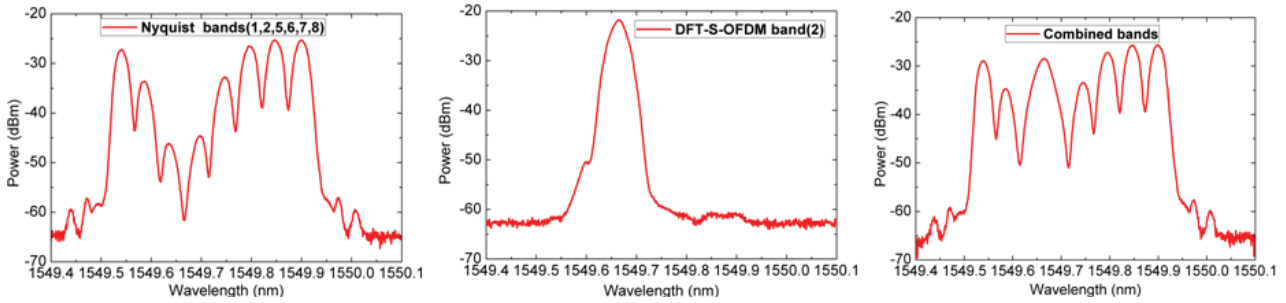

(a) (b) (c)

Fig. 8. Optical spectra of switching node: (a) Nyquist subbands (1, 2, 5, 6, 7, and 8), (b) DFT-S-OFDM subband (2), and (c) combined subbands.

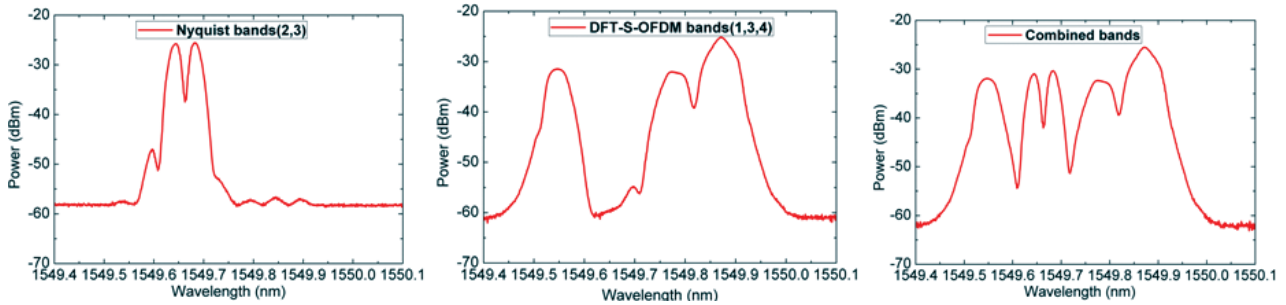

(a) (b) (c)

Fig. 9. Optical spectra of switching node: (a) Nyquist subbands (3 and 4), (b) DFT-S-OFDM subbands (1, 3, and 4), and (c) combined subbands.

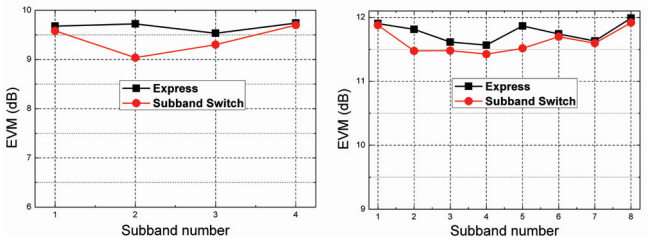

(a) (b)

Fig. 10. EVM values of each subband in switching path and express path: (a) DFT-S-OFDM superchannel and (b) Nyquist superchannel.

besides the required bands are much smaller compared to the required signals. Output of band-stop optical filters performed by Waveshaper 4000s is shown in Fig. 8(a) and 9(b). The residual signals on the suppressed bands are obvious, especially for Nyquist superchannel, because of the finite slope of filter. The difference of band-stop characteristic between two superchannel systems can be explained by more central density distributions for DFT-S-OFDM than Nyquist superchannel on a 12.5 GHz grid.

It can be observed that two Nyquist subbands are switched with one DFT-S-OFDM subband at the same frequency in a 12.5 GHz grid, as shown in Figs. 8(c) and 9(c). Figure 10 shows the comparison of express path with switching path on measured EVM values of each subband. We can observe the obvious EVM penalty for the DFT-S-OFDM band 2 because of the residual suppressed Nyquist band signals in Fig. 8(a) caused by band-stop waveshaper. The EVM penalty for the Nyquist bands 2 and 5 shown in Fig. 10 is caused by the imperfect filtering characteristics of band-stop optical filter. The OSNR of Nyquist bands 2 and 5 is reduced by the unflatness of optical filtering. The switching penalty for other subbands is less.

In conclusion, we experimentally show multigranularity optical subbands switching functionality between DFT-S-OFDM and Nyquist superchannels on a 12.5 GHz grid. We observe some EVM penalties for some bands due to the imperfect filtering characteristics of the optical filters. Optical switching functionality for individual band between different superchannels with multigranularity is feasible.

This work was supported by the National 973 Program of China (No. 2010CB328201), the National 863 Program of China (No. 2012AA011302), and the National Natural Science Foundation of China (No. 61077053). The authors also acknowledge the support from Program for New Century Excellent Talents in University.

References

1. Y. Tang, W. Shieh, and B. S. Krongold, IEEE Photon. Technol. Lett. **22**, 1250 (2010).
2. 3GPP TR 25.814, Physical layer aspect for evolved Universal Terrestrial Radio Access (UTRA) (2006).
3. Q. Yang, Z. He, Z. Yang, S. Yu, X. Yi, and W. Shieh, Opt. Express **20**, 2379 (2012).

4. F. Zhang, C. Yang, X. Fang, T. Zhang, and Z. Chen, Opt. Express **21**, 6115 (2013).
5. C. Zhao, Y. Chen, S. Zhang, J. Li, F. Zhang, L. Zhu, and Z. Chen, Opt. Express **20**, 787 (2012).
6. S. Sesia, I. Toufik, and M. Baker, *LTE—The UMTS Long Term Evolution. From Theory to Practice* (Wiley, 2009), Chap. 15.
7. Z. Zheng, R. Ding, F. Zhang, and Z. Chen, Opt. Express **21**, 17505 (2013).
8. X. Zhou, L. Nelson, P. Magill, R. Isaac, B. Zhu, D. W. Peckham, P. I. Borel, and K. Carlson, J. Lightwave Technol. **30**, 553 (2012).
9. R. Dischler, F. Buchali, and A. Klekamp, in *Proceedings of (OFC) 2010* 1 (2010).
10. Y. Chen, J. Li, C. Zhao, L. Zhu, F. Zhang, Y. He, and Z. Chen, IEEE Photon. Technol. Lett. **24**, 215 (2012).
11. R. Ding, Z. Zheng, R. Wang, T. Zhang, and F. Zhang, in *Proceedings of (OECC/PS) 2013* TuT2-4 (2013).
12. R. Ding and F. Zhang, in *Proceedings of (ACP) 2013* AW4F.4 (2013).
13. R. Schmogrow, B. Nebendahl, M. Winter, A. Josten, D. Hillerkuss, S. Koenig, J. Meyer, M. Dreschmann, M. Huebner, C. Koos, J. Becker, W. Freude, and J. Leuthold, IEEE Photon. Technol. Lett. **24**, 61 (2012).